Published in *IEEE Trans. Appl. Supercond.*, vol. 27, no. 4, June 2017. DOI: 10.1109/TASC.2016.2633301

Magnetic Shielding Above 1 T at 20 K With Bulk, Large Grain YBCO Tubes Made by Buffer-aided Top Seeded Melt Growth

L. Wéra, J. F. Fagnard, D. K. Namburi, Y. Shi, B. Vanderheyden and P. Vanderbemden

Keywords: High-temperature superconductors, Magnetic field, Magnetic shielding, YBCO.

Abstract

YBCO tubes of ~ 10 mm diameter closed at one extremity were engineered by a Buffer-Aided Top Seeded Melt Growth fabrication process (BA-TSMG). These tubes can act as efficient "dc" magnetic shields and are observed to reduce axial flux densities of 1.5 T by a factor of 100 at 20 K. Such performances are comparable in magnitude to the record threshold inductions reported for bulk MgB_2 and Bi-2212 materials at lower temperatures. Magnetic shielding measurements for open and closed tubes at 77 K also show that the presence of the cap improves substantially the shielding performance at the closed extremity since it reduces the penetration through the open end. This fabrication technique is extremely promising for shielding "dc" stray fields generated by HTS magnets operated in a temperature range obtained by cryocoolers, liquid hydrogen (20 K) or liquid neon (27 K).

Introduction

Several high sensitive scientific devices, e.g. superconducting quantum interference devices [1, 2], dc current transformers [3], or cryogenic current comparators [4], need to be protected against the magnetic field environment and therefore must be shielded. Superconducting materials are certainly the best candidates to build passive magnetic shields at low frequency. In a superconductor the shielding is provided by macroscopic currents loops flowing in the wall of the sample. The shielding effectiveness is characterized by two parameters: (i) the shielding factor (*SF*), defined here as the ratio between the applied magnetic induction and the local magnetic induction measured inside the shield, and (ii) the "threshold" or "limit" induction (B_{lim}), i.e. the applied magnetic induction above which a given value of the shielding factor cannot be achieved. Unlike ferromagnetic shields for which B_{lim} is intrinsically limited by the saturation magnetization (~ 2 teslas), superconductors have a priori much higher shielding potential [5], provided they can be manufactured (or assembled) in the form of a cavity. The recent increase of the performances of coated conductors used for high-field magnets [6, 7] will facilitate the emergence of superconducting devices operating at a few teslas, i.e. above the saturation of iron. There is an increasing need, therefore, to shield the considerable stray fields that results. In this paper we show that high field magnetic shielding can be achieved efficiently with bulk, large grain $YBa_2Cu_3O_7$ (YBCO) closed tubes when they are cooled in the range 20-40 K. This temperature range is accessible easily with closed-cycle coolers, liquid hydrogen (20 K) or liquid neon (27 K).

In a good approximation, the limit field B_{lim} is mainly determined by the product of the critical current density J_c and a geometrical dimension which, in most cases, is limited by the wall thickness d of the superconducting enclosure [8]. Films deposited on metallic substrates [9, 10] or structures made of coated conductors [11-14] have the advantage of being easily scalable but are not currently appropriate for shielding high fields because of their small thickness. Bulk cylinders made of high temperature superconductors (HTS), on the other hand, have already demonstrated their high-field shielding abilities. At T = 4.2 K, fields of the order of 1 T can be shielded with bulk MgB_2 [3, 15, 16] and efficient shielding up to 2 T was reported for a long MgB_2 cylinder [17]. These values are comparable to those achieved with using Nb-Ti multifilamentary composite wires at the same temperature [18]. At T = 10 K, bulk $Bi_2Sr_2CaCu_2O_8$ (BSCCO-2212) tubes can be used for shielding fields up to 1 T [19]. Solenoid magnets made of bulk melt-textured YBCO prepared by various techniques [20-26] show significant potential for magnetic shielding. There are very few reports, however,

describing their shielding performances. Sasaki *et al.* gave evidence of magnetic shielding of 0.2 T at 77 K with samples prepared by a modified Quench and Melt Growth process [20]. Fang *et al.* reported efficient shielding of the ambient noise [21]. Zhang *et al.* investigated the flux penetration through millimetric-size holes or gaps between YBCO bulks [27].

1. Experiment

1.1. Shield Geometry and Fabrication Process

For a hollow cylinder, it should be kept in mind that the best shielding performance levels are usually achieved at the center of the tube and decrease towards both extremities due to the field penetration through the open ends. This effect is more important in the case of a short tube. A way to solve this problem is to close the tube at one or both extremities by a superconducting cap [28, 29]. In the present case, our superconducting tube was fabricated by the Buffer-aided Top Seeded Melt Growth (BA-TSMG) process [30-32], in the Bulk Superconductivity Group at the University of Cambridge. This fabrication process enables the tube to be closed at one extremity by a cap containing the seed. Furthermore, as the cap and the tube are naturally welded together, there is no air gap between the cap and the tube.

Commercial powders of Y-123 (99.9 % pure, Toshima), Y-211 (99.9 % pure, Toshima) and CeO_2 (99.9 % pure, Alfa Aesar) were used as initial precursors. 25 wt % Y-211 and 0.5 wt % CeO_2 were added to the Y-123 powder and mixed together thoroughly using a mechanical mixer for 3 hours. CeO_2 was added to the precursor to refine the grain size of Y-211 inclusions in the fully processed single grain.

First, the mixed precursor powders of about 50 g were pressed uniaxially into long cylinder of 31 mm in diameter. Then, 6 g of the same powder was used to prepare a disc (25 mm in diameter) and was arranged on the top of the cylinder. This was further supported with the buffer pellet (of same composition, 5 mm diameter, 0.2 g). Finally, NdBCO seed crystal cleaved along (001) was placed on the top surface of the buffer pellet assembly as shown in Figure 1 (a). The melting process involved heating the samples to 1056 °C, holding for 1 hour to enable complete incongruent melting of the Y-123 phase into solid Y-211 and a liquid phase. Then, the sample was then cooled down rapidly to 1015 °C and then slowly cooled down at 0.8 – 0.2 °C/h to 978 °C to ensure heterogeneous nucleation and growth of the Y-123 phase. Finally, the sample was cooled to room temperature and the fully melt processed sample was annealed in flowing oxygen at 450 °C for 150 hours. Figure 1 (b) shows the final sample and Table 1 gives its average dimensions. In a second set of experiments, the cap was cut, resulting in a tube open at both ends.

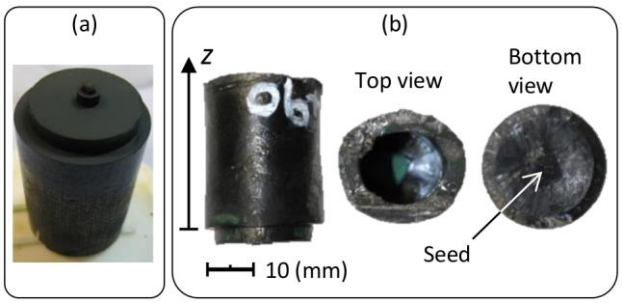

Figure 1. (a) The cylinder and the cap with the buffer layer and the NdBCO seed crystal placed on top of the arrangement prior to melt processing. (b) Picture of the final YBCO closed tube.

Table 1. Geometrical Characteristics of the YBCO Closed Tube.

Length of the tube	l = 30 mm
Inner radius (average)	r_1 = 7.4 mm
Outer radius (average)	r_2 = 11.8 mm
Wall thickness	$d = r_2 - r_1$ = 4.4 mm
Aspect ratio	l/r_2 = 2.54

1.2. Experimental Setups

Magnetic shielding properties were investigated using two different experimental setups. First, experiments were carried out in liquid nitrogen (77 K) using a miniature *Arepoc* Hall sensor that was moved along the axis of the tube. The tube was subjected to a uniform quasi static ("dc") magnetic field slowly ramped up to 60 mT at a constant sweep rate of 1 mT/s. Unlike other works where transverse [3, 8] or inhomogeneous fields [33] are investigated, a pure axial field is used in this study. Second, we characterized the superconducting shield at different temperatures using a *Physical Property Measurement System* (PPMS) instrumented with a Hall probe placed at the closed extremity of the tube. In this case, the tube was subjected to a uniform quasi static ("dc") magnetic field slowly ramped up to about 3 T (at 20 K) at a constant sweep rate of 0.33 mT/s.

2. Results and discussion

2.1. Shielding Properties at 77 K in Liquid Nitrogen

We first examine the experimental results obtained at 77 K. We compare the initial tube, closed at one extremity, with the open tube. Figure 2 shows the applied field dependence of the shielding factor $SF = B_{app}/B_z$ measured at three positions (every 15 mm) along the z axis of the tube, as sketched in the inset of Figure 2. For the closed tube, z = 0 corresponds to the closed extremity and z = 30 is the open extremity. The plain symbols correspond to the closed tube and the white symbols relate to the open tube.

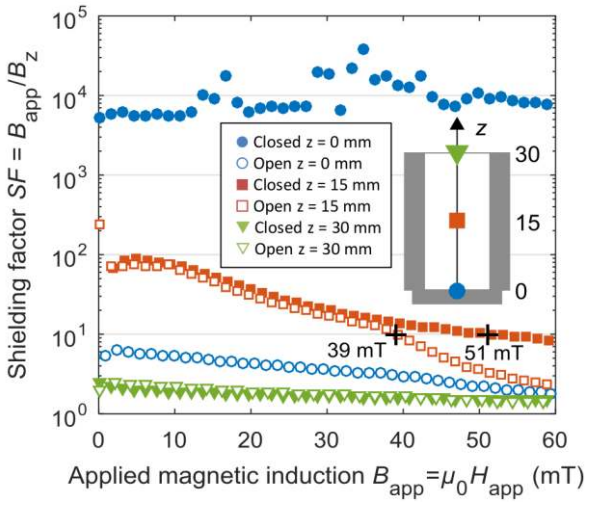

Figure 2. Shielding factor $SF = B_{app}/B_z$, as a function of the applied magnetic induction $B_{app} = \mu_0 H_{app}$, measured for three positions along the z axis of the tube. Plain symbols correspond to the closed tube and white symbols correspond to the open tube.

Figure 2 shows that the shielding factor at the closed extremity (plain circles) lies around 10^4 in the whole magnetic field range investigated (up to 60 mT). For the closed tube, the shielding factor decreases towards the open extremity (circles then triangles). For the open tube, the shielding factor is at maximum near the center and decreases towards both open extremities due to end effects.

The relatively small shielding factor at the center of the open tube can be explained by the small aspect ratio (l/r_2 = 2.54 where l is the length and r_2 is the outer radius) of the tube. In this case, the shielding factor at the center of the open tube is influenced by two field penetration mechanisms: the field penetration through the sample thickness but also by the open ends. This latter mechanism is predominant in the present case since simulations and experiments [28, 29] have shown that maximum shielding factor levels are reached at the center of a hollow cylinder for aspect ratios higher than 6.

At the center of the tube (z = 15 mm), the shielding factors for both open and closed tubes are similar up to 40 mT and then starts to diverge for higher fields. For SF = 10, a threshold induction B_{lim} of 39 mT is measured at the center of the open tube whereas for the closed tube, the threshold induction is 51 mT. This result gives evidence that the cap still has a beneficial influence at the center of the tube.

The threshold induction B_{lim} at the center of the open tube can be used to estimate the field-independent critical current density J_c. If we assume a uniform current density flowing on a macroscopic scale, the threshold induction for a tube of finite length l, thickness d and mean radius r_a, can be estimated by [34, 35]:

$$B_{lim} = \mu_0 J_C d \frac{l}{4r_a} \ln\left(\frac{4r_a}{l} + \sqrt{1 + \left(\frac{4r_a}{l}\right)^2}\right) \quad (1)$$

For B_{lim} = 39 mT, we obtain the average critical current density $J_c \approx 847$ A/cm². The value is smaller than that expected for single-grained YBCO samples in the form of disk pellets (of the order of 10^4 A/cm²), which can be ascribed to the fact that some parts of the tube are not perfectly textured especially those far away from the seed. This J_c value, however, is much higher than that obtained previously in polycrystalline YBCO [36] or BSCCO hollow cylinders (of the order of 350 A/cm² at 77 K and 20 mT [8, 19]). Knowing J_c, the threshold induction B_{lim} for a four times longer tube is estimated to be 47 mT, a value similar to the B_{lim} = 51 mT measured at the center of the closed tube.

Figure 3 shows the shielding factor $SF = B_{app}/B_z$ measured at seven positions (every 5 mm) along the z axis of the tube for a given applied magnetic field B_{app} = 30 mT, at 77 K.

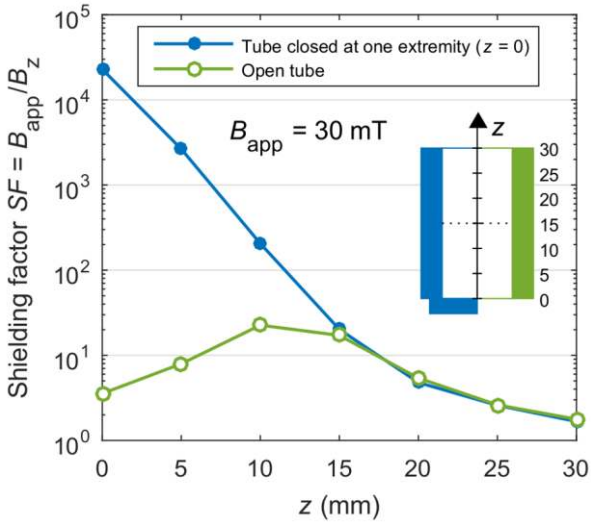

Figure 3. Shielding factor SF distribution measured at 77 K as a function of the position z of the Hall probe along the axis of the tube for B_{app} = 30 mT. z = 0 corresponds to the closed extremity.

For the closed tube, a shielding factor *SF* exceeding 10^4 was measured near the closed extremity ($z = 0$). Then the shielding factor decreases from the closed extremity to the open extremity. For the open tube, the shielding factor is maximum near the center of the tube and decreases towards both open extremities. A slight asymmetry of the shielding factor distribution with respect to the center of the tube ($z = 15$ mm) can be observed. This is consistent with the fact that the growth started from the cap (position $z = 0$). As a consequence, the critical current density can be assumed to be better near the closed extremity and within the cap than elsewhere in the tube. If we compare the closed and open tube configurations, we can see clearly that the cap increases significantly the shielding factor value at the closed extremity.

2.2. Shielding Properties at Various Temperatures

We now turn to the shielding behavior of the closed sample at various temperatures. Measurements are carried out at the closed extremity, where the best shielding factor levels have been observed at $T = 77$ K. Figure 4 shows the evolution of the shielding factor $SF = B_{app}/B_z$ at the closed extremity as a function of the applied magnetic induction $B_{app} = \mu_0 H_{app}$ for six different temperatures ranging from 20 K to 77 K. The inset shows the temperature dependence of the threshold induction B_{lim} at the closed extremity, defined for two shielding factors (10 and 100).

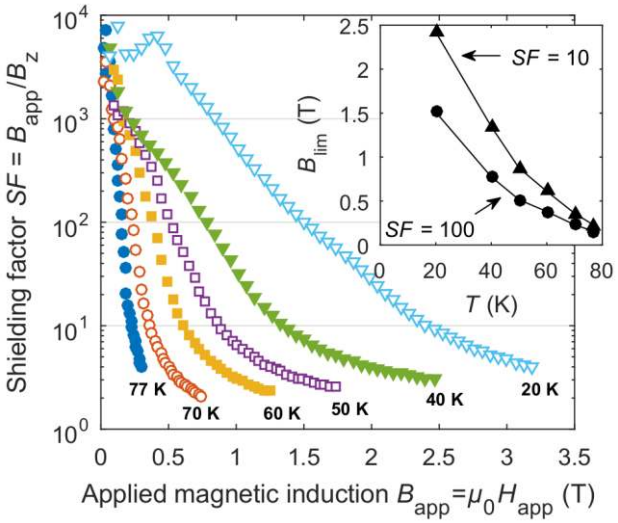

Figure 4. Shielding factor $SF = B_{app}/B_z$ at the closed extremity, as a function of the applied magnetic induction $B_{app} = \mu_0 H_{app}$ for temperatures ranging from 20 K to 77 K. Inset: temperature dependence of the threshold induction B_{lim} defined either for $SF = 10$ (triangles) or $SF = 100$ (circles).

The results plotted in Figure 4 show how the shielding factor increases as temperature decreases. For a given shielding factor, all curves are shifted to higher fields for decreasing temperatures. At low magnetic fields, the maximum shielding factor levels are found to remain between 10^3 and 10^4 for all temperatures. The inset of Figure 4 shows the temperature dependence of the threshold induction B_{lim} (defined for two shielding factors 10 and 100). The B_{lim} values measured at 77 K (respectively 155 mT [$SF = 100$] and 225 mT [$SF = 10$]) are found to be approximately 10 times higher at 20 K, i.e. 1.52 T [$SF = 100$] and 2.4 T [$SF = 10$]. In comparison, MgB_2 tubes were reported to shield axial magnetic inductions between 1 T [15] and 2 T [17] at 4.2 K. Additionally, melt casted BSCCO-2212 hollow cylinders were reported to shield magnetic inductions up to 800 mT at 20 K and 1 T at 10 K [19]. It is to be noted that the latter samples used for comparison have sizes similar to the magnetic shield investigated in this work, i.e. a useful inner diameter larger than 10 mm. Strictly speaking, shielding at higher field was reported in tiny holes or gaps in/between bulk superconductors [27], [37] (1-2 mm), but such small bores are clearly out of the scope of the present study.

Assuming a uniform J_c, we can expect that the shielding factor distribution at 20 K along the axis of the closed tube will have the same behavior as the distribution at 77 K. We can therefore estimate the threshold induction at the center of the closed tube at 20 K from the distribution at 77 K and the threshold induction measured at the closed end at 20 K. At 77 K, we know the ratio between the threshold inductions at the center of the tube and at the closed extremity. Under the previous assumption, this ratio should be the same at 20 K and we find a center threshold induction to be around 545 mT. Using the same procedure as before (Eq. (1)), the critical current density J_c at 20 K can be estimated to be 9×10^3 A/cm², under an average field in the superconductor approximated as half the applied field (~ 1.2 T).

In the present experiment, we purposefully avoid to submit the material to lower temperatures in order to avoid the occurrence of flux jumps which might be destructive [20]. If we consider a constant J_c, the maximum dissipated power at 20 K and for a fully penetrated tube is of the order of 1.2 mW, under the investigated 'quasi-static' sweep rate (0.33 mT/s). The associated rate of average temperature increase of the sample is of the order of 2×10^{-4} K/s, meaning that self-heating effects are insignificant. Finally, the threshold induction at a given temperature can be estimated by the following power-law:

$$B_{lim}(T) = B_{lim}(0)\left(1 - \frac{T}{T_C}\right)^{\delta} \quad (2)$$

where T_c = 93.5 K was obtained by a measurement of the trapped field of the cylinder as a function of the temperature. By fitting the B_{lim} values shown in the inset of Figure 4 we obtain $B_{lim}(0)$ = 2 T and δ = 1.5 for *SF* = 100 and $B_{lim}(0)$ = 3.2 T and δ = 1.6 for *SF* = 10. These parameters can be used to estimate the shielding threshold when the screen is operated at other temperatures, either accessible through closed-cycle coolers or liquid neon (27 K).

3. Conclusions

In conclusion, we have fabricated a YBCO tube made by Buffer-aided Top Seeded Melt Growth and characterized its high-field magnetic shielding performances. Thanks to the fabrication process, the tube is initially closed by a cap. We studied the initial tube, closed at one extremity by a cap containing the seed and the tube with the removed cap. The comparison of both configurations at 77 K showed that cap provides an important improvement of the shielding efficiency. At the center of the tube and towards the open extremity, a small difference on the shielding factor levels has been observed between both configurations. The characterization of the closed sample at various temperatures showed how the shielding efficiency increases for decreasing temperatures. In particular, threshold inductions of 1.5 T (for *SF* = 100) and 2.4 T (for *SF* = 10) were measured at 20 K, which is comparable to the threshold inductions measured for bulk MgB_2 and Bi-2212 hollow cylinders but at lower temperatures. The general conclusion is that these results give evidence that efficient magnetic shields can be obtained with this fabrication technique.

References

[1] Ohta H, Koike A, Hoshino K, Kotaka H, Sudoh E, Kato K, Takahara H, Uchikawa Y, Shinada K, Takahad M, Yamada Y and Matsuit T 1993 Neuromagnetic SQUID measurements in a helmet-type superconducting magnetic shield of BSCCO *IEEE Trans. Appl. Supercond.* **3**

[2] Kamiya K, Warner B A and DiPirro M J 2001 Magnetic shielding for sensitive detectors *Cryogenics* **41** 401

[3] Arpaia P, Ballarino A, Giunchi G and Montenero G 2014 MgB2 cylindrical superconducting shielding for cryogenic measurement applications: a case study on DC current transformers *Journal of Instrumentation* **9** P04020

[4] Giunchi G, Bassani E, Cavallin T, Bancone N and Pavese F 2007 An MgB2 superconducting shield for a cryogenic current comparator working up to 34 K *Superconductor Science and Technology* **20** L39-L41

[5] Durrell J H, Dennis A R, Jaroszynski J, Ainslie M D, Palmer K G B, Shi Y H, Campbell A M, Hull J, Strasik M, Hellstrom E E and Cardwell D A 2014 A trapped field of 17.6 T in melt-processed, bulk Gd-Ba-Cu-O reinforced with shrink-fit steel *Superconductor Science and Technology* **27** 082001

[6] Leroux M, Kihlstrom K J, Holleis S, Rupich M W, Sathyamurthy S, Fleshler S, Sheng H P, Miller D J, Eley S, Civale L, Kayani A, Niraula P M, Welp U and Kwok W K 2015 Rapid doubling of the critical current of YBa2Cu3O7−δ coated conductors for viable high-speed industrial processing *Applied Physics Letters* **107** 192601

[7] Trociewitz U P, Dalban-Canassy M, Hannion M, Hilton D K, Jaroszynski J, Noyes P, Viouchkov Y, Weijers H W and Larbalestier D C 2011 35.4 T field generated using a layer-wound superconducting coil made of (RE)Ba2Cu3O7−x (RE = rare earth) coated conductor *Applied Physics Letters* **99** 202506

[8] Fagnard J F, Dirickx M, Ausloos M, Lousberg G, Vanderheyden B and Vanderbemden P 2009 Magnetic shielding properties of high-Tc superconducting hollow cylinders: model combining experimental data for axial and transverse magnetic field configurations *Superconductor Science and Technology* **22** 105002

[9] Pavese F, Bergadano E, Bianco M, Ferri D, Giraudi D and Vanolo M 1997 *Advances in Cryogenic Engineering Materials,* ed L T Summers (Boston, MA: Springer US) pp 917-22

[10] Kumar N D, Closset R, Wera L, Cloots R, Vanderbemden P and Vertruyen B 2015 Magnetic shielding performances of YBa2Cu3O7−δ-coated silver tubes obtained by electrophoretic deposition *Superconductor Science and Technology* **28** 015007

[11] Fagnard J F, Dirickx M, Levin G A, Barnes P N, Vanderheyden B and Vanderbemden P 2010 Use of second generation coated conductors for efficient shielding of dc magnetic fields *Journal of Applied Physics* **108** 013910

[12] Wéra L, Fagnard J F, Levin G A, Vanderheyden B and Vanderbemden P 2013 Magnetic Shielding With YBCO Coated Conductors: Influence of the Geometry on Its Performances *IEEE Trans. Appl. Supercond.* **23** 8200504

[13] Tomkow L, Ciszek M and Chorowski M 2015 Combined magnetic screen made of Bi-2223 bulk cylinder and YBCO tape rings—Modeling and experiments *Journal of Applied Physics* **117** 043901

[14] Kvitkovic J, Davis D, Zhang M and Pamidi S 2015 Magnetic Shielding Characteristics of Second Generation High Temperature Superconductors at Variable Temperatures Obtained by Cryogenic Helium Gas Circulation *IEEE Trans. Appl. Supercond.* **25** 8800304

[15] Cavallin T, Quarantiello R, Matrone A and Giunchi G 2006 Magnetic shielding of MgB2 tubes in applied DC and AC field *Journal of Physics: Conference Series* **43** 1015

[16] Gozzelino L, Gerbaldo R, Ghigo G, Laviano F, Truccato M and Agostino A 2016 Superconducting and hybrid systems for magnetic field shielding *Superconductor Science and Technology* **29** 034004

[17] Rabbers J J, Oomen M P, Bassani E, Ripamonti G and Giunchi G 2010 Magnetic shielding capability of MgB2 cylinders *Superconductor Science and Technology* **23** 125003

[18] Takahata K, Nishijima S, Ohgami M, Okada T, Nakagawa S and Yoshiwa M 1989 Magnetic shielding by a tubular superconducting winding in parallel and transverse fields *IEEE Trans. Magn.* **25** 1889-92

[19] Fagnard J F, Elschner S, Bock J, Dirickx M, Vanderheyden B and Vanderbemden P 2010 Shielding efficiency and E(J) characteristics measured on large melt cast Bi-2212 hollow cylinders in axial magnetic fields *Superconductor Science and Technology* **23** 095012

[20] Sasaki T, Tanaka M, Morita M, Miyamoto K and Hashimoto M 1992 Magnetic Shielding by Superconducting Y-Ba-Cu-O Prepared by the Modified Quench and Melt Growth (QMG) Process *Japanese Journal of Applied Physics* **31** 1026-32

[21] Fang H, Claycomb J R, Zhou Y X, Putman P T, Padmanabhan S, Miller J H, Ravi-Chandar K and Salama K 2003 Melt-textured YBCO superconducting tube for magnetic shielding *IEEE Trans. Appl. Supercond.* **13** 3103-5

[22] Withnell T D, Babu N H, Majoros M, Reddy E S, Astill D M, Shi Y, Cardwell D A, Campbell A M, Kerley N and Zhang S 2005 Trapped field in individual and stacked rings of bulk melt processed Y-Ba-Cu-O *IEEE Trans. Appl. Supercond.* **15** 3125-8

[23] Scruggs S J, Putman P T, Fang H, Alessandrini M and Salama K 2006 Growth techniques for monolithic YBCO solenoidal magnets *Physica C: Superconductivity and its Applications* **445–448** 312-6

[24] Shi Y, Dennis A R, Xu Z, Campbell A M, Hari Babu N and Cardwell D A 2010 Field trapping of Y–Ba–Cu–O single grain rings joined to form the geometry of a solenoid *Superconductor Science and Technology* **23** 045014

[25] Tomita M, Fukumoto Y, Suzuki K, Ishihara A and Muralidhar M 2011 Development of a compact, lightweight, mobile permanent magnet system based on high Tc Gd-123 superconductors *Journal of Applied Physics* **109** 023912

[26] Nariki S, Teshima H and Morita M 2016 Performance and applications of quench melt-growth bulk magnets *Superconductor Science and Technology* **29** 034002

[27] Zhang Z Y, Matsumoto S, Teranishi R and Kiyoshi T 2012 Magnetic shielding properties of GdBCO bulks with different crystal orientation *Physics Procedia* **27** 180-3

[28] Denis S, Dirickx M, Vanderbemden P, Ausloos M and Vanderheyden B 2007 Field penetration into hard type-II superconducting tubes: effects of a cap, a non-superconducting joint, and non-uniform superconducting properties *Superconductor Science and Technology* **20** 418-27

[29] Wéra L, Fagnard J F, Hogan K, Vanderheyden B and Vanderbemden P 2016 *Superconductivity: Applications Today and Tomorrow* ed M Muralidhar (New York: Nova Science) pp 95-114

[30] Devendra Kumar N, Shi Y, Zhai W, Dennis A R, Durrell J H and Cardwell D A 2015 Buffer Pellets for High-Yield, Top-Seeded Melt Growth of Large Grain Y–Ba–Cu–O Superconductors *Crystal Growth & Design* **15** 1472-80

[31] Namburi D K, Shi Y, Palmer K G, Dennis A R, Durrell J H and Cardwell D A 2016 An improved top seeded infiltration growth method for the fabrication of Y–Ba–Cu–O bulk superconductors *Journal of the European Ceramic Society* **36** 615-24

[32] Namburi D K, Shi Y, Palmer K G, Dennis A R, Durrell J H and Cardwell D A 2016 Control of Y-211 content in bulk YBCO superconductors fabricated by a buffer-aided, top seeded infiltration and growth melt process *Superconductor Science and Technology* **29** 034007

[33] Hogan K, Fagnard J F, Wéra L, Vanderheyden B and Vanderbemden P 2015 Magnetic shielding of an inhomogeneous magnetic field source by a bulk superconducting tube *Superconductor Science and Technology* **28** 035011

[34] Denis S, Dusoulier L, Dirickx M, Vanderbemden P, Cloots R, Ausloos M and Vanderheyden B 2007 Magnetic shielding properties of high-temperature superconducting tubes subjected to axial fields *Superconductor Science and Technology* **20** 192-201

[35] Navau C, Sanchez A, Pardo E, Chen D X, Bartolomé E, Granados X, Puig T and Obradors X 2005 Critical state in finite type-II superconducting rings *Physical Review B* **71**

[36] Symko O G, Yeh W J, Zheng D J and Kulkarni S 1989 Magnetic shielding and relaxation characteristics of superconducting YBa2Cu3O7 tubes *Journal of Applied Physics* **65** 2142

[37] Lousberg G P, Fagnard J F, Haanappel E, Chaud X, Ausloos M, Vanderheyden B and Vanderbemden P 2009 Pulsed-field magnetization of drilled bulk high-temperature

superconductors: flux front propagation in the volume and on the surface *Superconductor Science and Technology* **22** 125026